

Research on Engineering Structures & Materials



www.jresm.org

Research Article

Experimental study on strengthening compression members with recycled aggregate concrete using FRP techniques

Sastri M.V.S.S*,1,a, N.R. Dakshina Murthy 2,b, L. Sudheer Reddy 3,c, S. Vijaya Kumar 1,d

- ¹Dept. of Civil Eng., Vasavi College of Engineering (A), Hyderabad, Telangana, India
- ²Dept. of Civil Eng., Chaitanya Bharathi Institute of Technology (A), Hyderabad, Telangana, India
- ³Dept. of Civil Eng., Kakatiya Institute of Technology & Science (A), Warangal, Telangana, India

Article Info

Article History:

Received 23 July 2025 Accepted 11 Nov 2025

Keywords:

Epoxy resin; Fibre reinforced polymer sheets; Passive confinement; Recycled aggregate; Stress-strain

Abstract

This study investigates the axial behavior of recycled aggregate concrete (RAC) cylinders (150 × 300 mm, 50 % recycled coarse aggregate) strengthened using external fibre-reinforced polymer (FRP) wraps: carbon (CFRP), basalt (BFRP), and glass (GFRP) combined with internal steel ties to form a hybrid confinement system. Nine mix configurations were tested to evaluate the influence of FRP type and tie spacing on compressive strength, ductility, and confinement efficiency. Recycled aggregates led to a 10-13 per cent decrease in the natural compressive strength at the base level owing mainly to their different microstructure and increased water absorption. The experimental results show that hybrid confinement markedly improves the mechanical performance of RAC. Compared with unconfined specimens (30.2 MPa), FRP-only systems increased compressive strength by 40-100 %, while the inclusion of three and four steel ties further enhanced it by 60-80 %. The ultimate axial strain rose by as much as twelve times (≈1200 %), indicating substantial gains in deformability and energy absorption. The strength hierarchy CFRP > BFRP > GFRP was consistent across all tie configurations, though the performance gap narrowed as tie spacing decreased, confirming that volumetric steel ratio becomes dominant in highly confined systems. Analytical predictions using the modified Lam-Teng bilinear model correlated strongly with experimental strengths ($R^2 = 0.94$) but over-predicted strain due to RAC heterogeneity and premature FRP-epoxy debonding. Cost analysis identified BFRP as the most efficient material, providing ≈ 90 % of CFRP's performance at 50 % lower cost (₹ 24.5 / MPa vs ₹ 35 / MPa). The findings offer practical guidance for designing economical, high-ductility hybrid confinement systems for sustainable rehabilitation and retrofitting of structural members incorporating recycled aggregates.

© 2025 MIM Research Group. All rights reserved.

1. Introduction

Concrete is a fundamental construction product around the globe, and it is the foundation of the construction of buildings, structures, and infrastructure. Nevertheless, it has been heavily reliant on natural aggregates, a factor that has drawn grave environmental controversies such as depletion of resources and increased CO_2 emissions. Recycled aggregate concrete (RAC) in its turn is a sustainable alternative that has attracted growing research interest, produced out of construction and demolition wastes. However, RAC normally has a greater porosity, greater water retention and lesser interfacial transition zones, and thus, lower compressive strength as opposed to natural aggregate concrete (NAC) [1].

*Corresponding author: mvss.sastri@staff.vce.ac.in

dorcid.org/0000-0002-1701-5597

DOI: http://dx.doi.org/10.17515/resm2025-1040ma0723rs

Res. Eng. Struct. Mat. Vol. x Iss. x (xxxx) xx-xx

To overcome these shortcomings the use of fibre-reinforced polymer (FRP) confinement systems, including carbon fibre (CFRP), basalt fibre (BFRP), and glass fibre (GFRP) fibre-reinforced polymer, as strengthening and retrofitting. FRPs offer passive confinement, which increases compressive strength, ductility and strain capacity. However, the synergistic effect of FRP confinement and RAC is not properly investigated. The interaction between internal steel ties and external FRP wraps has rarely been studied in the past, and few studies have been able to come up with analytical models that can effectively predict the behavior of FRP-confined RAC [2, 3].

This research gap is filled by the current study conducted with experimental introspection of the RAC cylinders (50 percent recycled coarse aggregates) which are encircled by various FRP wraps (GFRP, BFRP, and CFRP) with and without internal steel ties. It also compares predictive accuracy of an enhanced Lam and Teng model [4] specific to the nonlinear predictive response of hybrid-confined RAC. The hybrid confinement method of combining internal and external confinement and model modification is the innovation and increase the prediction accuracy of the RAC systems.

1.1 Research Hypothesis

The hybrid confinement system consisting of internal steel ties with external FRP wraps will greatly enhance the compressive strength, ductility and strain capacity of RAC as compared to confinement systems of a single type. The improved Lam-Teng model will provide better predictive performance, which will be used in making reliable analytical instruments and sustainable structural strengthening mechanisms.

1.2 Objectives

- Compare mechanical properties of natural and recycled aggregates and their effect on the behavior of concrete.
- Test the impact of aggregate replacement as a percentage of the total on compressive behavior of FRP-confined RAC.
- Measure the predictive ability of the Lam and Teng model modified.
- Contribute to a sustainable strengthening with hybrid FRP confinement.

1.3 Literature Review

The study of the mechanical and durability of recycled aggregate concrete (RAC) has been conducted recently as a method of sustainable construction. Compressive strength and stiffness are normally low in RAC. Brendt [5] also showed that when 50 percent of the cement was replaced by ground-granulated blast furnace slag, RAC increased its durability and strength, better than fly ash, which is the contribution of other cementitious materials. Verian et al. [6] discovered that the properties of recycled coarse aggregates are dependent on the quality of source concrete and crushing process. Their experiment revealed that fly ash mixes of 20 percent enhanced compressive strength of 28 days by 10 percent and 5 percent in 50 and 100 percent RAC respectively. RAC axial and flexural performance limitations of RAC have also been studied. Xu et al. [7] demonstrated that the water absorption and pore structure influence the axial compressive behavior of RAC, especially when transverse reinforcement spacing is increased. In mix design and confinement, Choi and Yun [8] discovered that ACI code predictions can be used in the case of RAC columns in the uniaxial compression. Shatarat et al. [9] observed that compressive strength is reduced significantly above 20 percent RAC replacement and this is a limit that can be considered in practice.

Recognizing these limitations, researchers have explored several strategies to enhance RAC's performance and efforts to mitigate the limitations of RAC include fibre-reinforced polymer (FRP) confinement, which enhances compressive strength and ductility. Wang et al. [10] demonstrated that flexural strength of concrete-filled steel tubes was enhanced by carbon fibre-reinforced polymer (CFRP) wrapping. Wang et al. [11] experimented on CFRP-wrapped columns of RAC, which exhibited an increase in the axial capacity but slight improvements relative to natural aggregate concrete (NAC). According to Choudhury et al. [12], NAC was more successful at uniform confinement of the pressure in the circular sections. Suhail et al. [13] and Hadi Muhammad et al. [14] compared CFRP and shape-memory alloy (SMA) spirals confinement with CFRP being

stronger. Basalt fibre-reinforced polymers (BFRP) is moderately strong and energy dissipating. Abu-Sena et al. [15] established that CFRP wrapping put off local buckling in hollow columns. Kim et al. [16] reported decreasing properties as more plastic was recycled. Zhu et al. [17] found that CFRP-reinforced frames were more apt to exhibit increased ductility whereas Park et al. [18] demonstrated that the tighter the CFRP strips the fewer voids and bonded area is more considerable than strip width or layers.

The variables that influence compressive strength of RAC in the presence of FRP confinement have been evaluated. Silva et al. [19] highlighted the replacement ratio, aggregate size, moisture content and variability in RAC to be among the key factors. Xu et al. [7] discovered that when compressive strength was reduced and stress distribution changed more water was absorbed in RAC. Dey et al. [20] noticed reduced sizes had superior confinement response with RAC demonstrating superior strain at the expense of peak strength when compared to NAC. Zhao et al. [21] reported good predictions of compressive strength and underestimated ultimate strain in FRP confined RAC. Sunayana et al. [22] discovered that partial replace cement with fly ash increased the peak loads in the RAC column and the ACI models were less rigid than the Indian codes. According to Chen et al. [23], size effects were identified in GFRP-confined square RAC columns. Deresa et al. [24] have also noted the presence of similar crack patterns in RAC and NAC columns, but RAC was found to be less stiff and had lower load capacity. Zhang et al. [25] demonstrated that CFRP led to higher fracture energy of RAC beams, and Wu et al. [26] also reported that CFRP was confined in the use of GFRP. On the basis of 800 tests, Ozbakkaloglu and Lim [27] developed a better model of predicting the strain capacity of FRP-confined concrete, including RAC.

More closely attempting to predict the above-discussed outcomes, artificial intelligence (AI) and hybrid modelling have recently been introduced to predict the behavior of fibre-reinforced polymer (FRP)-confined recycled aggregate concrete (RAC). In their study, Khodadadi et al. [28] used CatBoost with the particle swarm optimization to forecast the strength of carbon fibrereinforced polymer (CFRP)-confined concrete to a high degree of precision. Dada et al. [29] designed a stress-strain response simulator of FRP-confined RAC/Natural aggregate concrete (CATO-MZW) that is superior to the traditional analytical formulations. On the same note, Nguyen et al. [30] have utilized AI algorithms to determine flexural behavior of CFRP sheet-reinforced RAC beams and secured a close rate of agreement with experimental results, whereas Neupane et al. [31] have used Random Forest and XGBoost to forecast flexural strength in RAC with fly ash, silica fume, and CFRP, and found that the Random Forest model is the best predictor. Taken together, the studies indicate that ensemble and hybrid AI models can achieve substantial prediction accuracy and interpretability of FRP confined RAC relative to empirical or semi-empirical methods. Nevertheless, their inference is limited by narrow, non-standardized data of RAC specific experiments that are inconsistent between aggregates, replacement ratios and testing procedures. Such a lack limits the strength of AI predictions and cross-study cross-validation. To address these shortcomings, Zhang et al. [32] developed a Bayesian-optimized ML model that was trained on RAC data only, whereas Al-Sharari et al. [33] provided a feature analysis of SHAP, which was used to determine the predominant mechanical parameters that can be used to control FRP-confined RAC behavior.

Other than studying the mechanical properties, durability and service life of RAC in harsh environment is important. Crumb rubber has also been explored in order to increase the resistance to chloride penetration and freeze-thaw cycles, but this decreases compressive strength [34]. Adding to the material changes, Harikrishna et al. [35] investigated the mechanical and durability properties of blended concrete with 25 percent fly ash and different RAC ratios (0-100 percent) and discovered that the blended concrete showed the best results with 25 percent fly ash and 75 percent RAC, yet the latter enhanced carbonation and minimized the corrosion resistance. When dealing with fire aspects in durability, Haris et al. [36] conducted a review of the fire behavior of FRP-strengthened members where deterioration of properties was being observed at high temperature and how fireproof design considerations were important. Mineral additions, which include micro silica and marble powder, have been found to lower the permeability of the self-compacting concrete in terms of permeability [37]. Asma et al. [38] utilized the Life-365 models to determine the advantages of admixtures in chloride-saturated conditions to determine their long-

term durability. With the emphasis on the design accuracy, Gedik [39] evaluated FRP-wrapped concrete guidelines and determined that most of their models were incorrect and suggested more realistic design methods. Based on environmental implication, basalt fibre-reinforced polymers (BFRP) have been considered as good alternatives due to their reduced environmental footprint compared to the CFRP [40, 41]. In order to sustain construction, Xing et al. [42] showed less embodied energy using the circular economy. Moreover, Fan et al. [40] have mentioned that BFRP/PVC-jacketed reinforced concrete (RAC) columns were highly efficient with minimal cost to the environment. With such improvements, a study on the long-term stability of the effect of UV exposure, aging of resin, and freeze-thaw degradation is still scarce [20, 21]. In general, this modern research confirms, once again, that the enhancement of performance in RAC should be measured along with the environmental indicators and the reliability of digital-modelling, and the current study explicitly incorporates such direction.

An integration of the articles reviewed has demonstrated that:

- It is inherently a drawback of RAC in comparison to NAC in terms of strengths and hardness that it is porous and possesses a weak bonding strength.
- FRP confinement, particularly CFRP and BFRP, always improves compressive, ductile, and energy absorption capacities of RAC structural members.
- The most important parameters, which influence the performance outcomes, include RAC content, aggregate quality, section geometry, and confinement configuration.
- AI-based modelling is becoming more relevant in complementing experimental research and enabling more realistic predictions of the FRP-confined RAC behavior.
- Issues of durability including ingress of chlorides, freeze thaws cycles and fire resistance are other areas which require further systematic research particularly when the site is in service.

1.4 Knowledge Gaps and Research Contribution

Although a lot of research has been conducted on the confinement of NAC by FRP, the mechanics, modelling and response of FRP-confined RAC, has limited insight on its confinement durability. Key gaps include:

- Poor strain prediction of current predictive models owing to un-modeled RAC dilation and bond heterogeneity.
- There is a lack of experimental data on hybrid confinement systems (FRP + steel ties) to assist with calibration of the model.
- The scarcity and irregularity of data are barriers to the generalization of AI models in the case of RAC.
- Absence of combined evaluation systems of performance and sustainability indicators.

The current research will fill these gaps by:

- Systematic experiments were performed on 50 % RAC cylinders enclosed with dissimilar Types of FRP (CFRP, BFRP, GFRP) with and without inner ties.
- Calibrating a modified Lam-Teng model to the parameters of a RAC.
- Offering an authentic dataset to future prediction frameworks based on ML.
- Providing supports towards formulating sustainable strengthening strategies, with the balance of performance, cost, and environmental impact.

Such a combined strategy will not only promote the knowledge of FRP-RAC hybrid confinement mechanisms but also it will provide insights into future data-oriented design models capable of providing reliable information to lead to sustainable structural retrofitting.

2. Materials and Methods

2.1 Materials Used

Cement: OPC 53 grade cement satisfying IS 269[43] was used. The properties were tabulated in Table 1.

Table 1. Properties of cement

Specific gravity	Fineness by sieve	Initial setting	Final setting	Normal
	analysis	time(mins)	time(mins)	consistency
3.014	2.05 %	30mins	360mins	33 %

- Fine aggregate: Locally available river sand confirming to IS 383[44] zone 2 was used.
- Natural coarse aggregate (NCA): Crushed granite stones passing through 20mm and retaining on 4.75 mm sieve was used satisfying IS 383[44].
- Recycled coarse aggregate (RAC): PCC cubes were crushed in jaw crusher, sieved, grinded and washed was used [44]. The properties were listed in Table 2. The RAC had adhered mortar (20–25 %) and was pre-soaked for 24 h and brought to a surface-saturated-dry condition before mixing. No additional water was added; thus, the effective w/b ratio = 0.45 was maintained for both NAC and RAC. This procedure minimizes variability caused by moisture imbalance, a key issue in RAC mixes.

Table 2. Properties of NCA and RAC

Test	Sp.	Bulk	Water	Impact	Fineness	Los Angeles
	Gravity	density	absorption	value	modulus	abrasion test
NCA	2.77	1440	0.6 %	35.6 %	7.51	29.2 %
RAC	2.53	1370	4.95 %	37.96 %	7.16	30.14 %

• Lateral ties: 8 mm diameter Fe 500 TMT steel lateral and 2mm wires were employed to hold the tie reinforcement in position. A clear cover of 25mm was maintained and the Volumetric ratio (ps) and the effective confinement pressure is 5 MPa (3 ties) and 7.9 MPa (4 ties), which was quantified as the difference between the compressive strength of tied and untied specimens by following the approach consistent with the confinement model of Mander et al. [45] and later it was adopted in FRP confinement studies [4, 46].

Table 3. Properties of ties

No. of ties	Spacing (mm)	Volumetric ratio ρs (%)	fl, steel (MPa)
3	100	2.19	5.4
4	66.7	3.25	8.2

2.1.1 Fibre Reinforced Polymer (FRP)

Three different types of FRP sheets comprising of Glass, Basalt and carbon fibre were used. Properties were shown in Table 3, and the properties of Epoxy Resin were shown in Table 4 and Fig. 1.

Table 4. Properties of Glass fabric (GFRP), Basalt fabric (BFRP), Carbon fabric (CFRP) as given by supplier

Fibre	Yield strength (MPa)	Density (g/cm³)	Thickness (mm)	Tensile strength (MPa)	$ \varepsilon_{fu} $ ultimate tensile strain	Sp. Gravity	Strain at break %	E-GPa	Cost (Rs.)
Carbon	1755-	1.55-	0.17	1720-	0.01	1-1.1	0.5-	230	3500/S
Garbon	3600	1.76	0.17	3690	0.01	1 1.1	1.9	_00	q.m
Basalt	1000-	2.15-	0.15	1035-	0.017	2.7-	1.6-	75	1800/
Dasait	1600	2.70	0.13	1650	0.017	2.89	3.0	73	Sq.m
E-glass	600-	2.11-	0.23	480-	0.021	1.5-2.5	1.2-	50	540/Sq.
	1400	2.70	0.23	1600	0.021	1.5-2.5	3.1	30	m



Fig. 1. Samples of GFRP, BFRP, CFRP sheets and Epoxy resin

2.1.2 Epoxy Resin

It is a viscous liquid that provides good pigment wetting for fibre fabrics with high mechanical and chemical resistance properties. Epoxy resin was applied to the surface of the structure, and then the fibre fabric was wrapped around it. The epoxy acts as an adhesive, holding the fibres securely to the concrete surface. Araldite 230-1 and Aradur HY 951L556 were mixed to obtain resin. The properties are listed in Table 4, and the sample figures of the materials are shown in Fig. 1. The Orientation of fibres is in hoop direction and overlap length 100 mm was maintained as per the ACI 440.2R-17[47].

Table 5. Properties of epoxy resin

S.No.	Properties	Epoxy Resin	Hardener
1	Appearance	Light yellow	Clear liquid
2	Company	Araldite L 556	Araldite H 951
3	Sp. Gravity	1.15-1.18	0.98+- 0.1
4.	Max viscosity at 270C	650+	/-100
5	Storage stability	12 months	6 months
6	Pot life @ 270C	1.5-2	hours

2.2 Preparation of Test Specimens

For each mix–confinement configuration, a total of four 150×300 mm cylinders were cast. Of these, three cylinders were tested in uniaxial compression to determine the average compressive strength (f'cc), while one additional companion cylinder was instrumented with a compress meter (200 mm gauge length) for the complete stress–strain response. The mean and standard deviation of strength values were computed from the three replicates, and the strain data from the instrumented specimen were taken as representative of the group.

The mix design followed IS:10262 [48] for M30 concrete with a constant water–binder ratio of 0.45 to maintain consistency between natural and recycled mixes (Table 6). The recycled aggregate concrete was prepared using $50\,\%$ natural and $50\,\%$ recycled aggregates. Reinforcement of natural and recycled aggregate concrete 8 mm diameter lateral ties were used. The cast concrete was removed from the moulds after $24\,\mathrm{h}$ and stored in a curing tank for $28\,\mathrm{days}$. After curing, FRP sheets were wrapped around the samples.

The parameters chosen in this experimental program were carefully selected to ensure both scientific relevance and practical applicability. The recycled aggregate replacement ratio was fixed at $50\,\%$ based on earlier findings that this level achieves an optimal balance between sustainability and structural integrity. Lower replacement ratios (less than $30\,\%$) offer limited environmental benefit, while higher proportions (more than $70\,\%$) significantly compromise strength and stiffness due to the weak interfacial transition zone (ITZ) and adhered mortar in recycled aggregates. The $50\,\%$ ratio thus reflects a realistic, field-applicable threshold recommended by Silva et al. [19] and Dey et al. [20].

Table 6. Mix design of M-30 grade concrete

Mix proportions	Cement	Fine	Coarse ag	gregates	atan	Fresh	Air	Slump (mm)	
		aggregates	NCA	RAC	water	(kg/m ³)	Density Content [kg/m³) (%)		
	NCA	378.95kg	560kg	1105.5kg	-	170.5	2390	2.0	95
	RAC	378.95kg	560.26 kg	552.7kg	511.6kg	liters	2360	2.2	90

The number of FRP layers was fixed at two after a preliminary trial program and review of ACI 440.2R-17 [47], which suggests that two layers generally mobilize effective confinement without excessive stiffness or premature FRP rupture. The fibre orientation was maintained strictly in the hoop direction, as lateral confinement governs axial compression resistance. The layer thicknesses 0.17 mm (CFRP), 0.15 mm (BFRP), and 0.23 mm (GFRP) were adopted from manufacturer data and aligned with the confinement assumptions of Teng et al. [4].

The specimen matrix (Table 7) was designed to evaluate the combined influence of confinement type and intensity, including FRP-only, steel-tie-only, and hybrid systems (three and four lateral ties). This factorial design ensured a systematic comparison of confinement mechanisms.

Table 7. Specimen Matrix

Group ID	Mix	Ties	FRP wrap (layers)	Specimen ID	n	f'cc(peak) (MPa) ±S.D.	Strain x 10 ⁻³ mm/m m	Notes
0T-N-U	NAC (100 %)	0	none	N-0	3	34.3±0.9	2.456	Unconfined NAC baseline
0T-R-U	RAC (50 %)	0	none	R-0	3	30.2±0.9	2.177	Unconfined RAC baseline
0T-R-G	RAC (50%)	0	GFRP (2 L)	R-G	3	42.4±1.0	1.403	FRP-confined only
0T-R-B	RAC (50 %)	0	BFRP (2 L)	R-B	3	52.2±2.0	4.426	_
0T-R-C	RAC (50 %)	0	CFRP (2 L)	R-C	3	60.2±1.3	1.748	_
3T-N-U	NAC (100%)	3	none	3N-C	3	38.0±1.3	8.989	Ties only (s = 100 mm)
3T-R-U	RAC (50%)	3	none	3R-U	3	33.2±1.2	9.018	Ties only (s = 100 mm)
3T-R-G	RAC (50%)	3	GFRP (2 L)	3R-G	3	67.7±2.0	18.58	Hybrid steel + GFRP
3T-R-B	RAC (50%)	3	BFRP (2 L)	3R-B	3	74.9±2.8	21.66	_
3T-R-C	RAC (50%)	3	CFRP (2 L)	3R-C	3	80.6±1.4	27.49	_
4T-N-U	NAC (100%)	4	none	4N-C	3	40.8±0.2	4.734	Ties only (s = 67.5 mm)
4T-R-U	RAC (50%)	4	none	4R-U	3	33.3±1.1	5.164	Ties only (s = 67.5 mm)
4T-R-G	RAC (50%)	4	GFRP (2 L)	4R-G	3	72.7±1.5	5.798	Hybrid steel + GFRP
4T-R-B	RAC (50%)	4	BFRP (2 L)	4R-B	3	77.7±1.1	12.59	_
4T-R-C	RAC (50%)	4	CFRP (2 L)	4R-C	3	84.7±2.5	27.97	

The Epoxy resin was wrapped around the cylinders using the following simple steps: The outside surface was smoothened using sandpaper. A primer coat mixture containing Araldite 230-1 and Aradur HY 951L556 was applied using a brush, and then the roller was used to remove the air bubbles between the concrete surface and the FRP fabric. The process is done on another layer totaling two numbers (Fig. 2 and 3). All specimens were water cured for 28 days at an ambient temperature of 27 ± 2 °C and relative humidity of 65-70 %. Following FRP wrapping, the epoxy resin was allowed to cure for 7 days at 25-30 °C before testing to ensure complete polymerization and stable bond formation. The Coupon tensile tests are reported from the supplier data; tensile strength 1.72-3.69 GPa (CFRP), 1.035-1.65 GPa (BFRP) and 0.48-1.6 GPa (GFRP). Due to equipment

limitations, direct tensile tests of FRP coupons were not conducted. Instead, supplier-certified data for tensile strength, rupture strain, and modulus were adopted per ACI 440.2R [47]. While this approach satisfies code compliance, supplier data often represent ideal laboratory curing conditions and may not capture in-situ resin variability. This reliance introduces limited uncertainty in confinement pressure and strain predictions. Future work will address this limitation by conducting direct FRP tensile and bond strength characterization to refine confinement coefficients and improve hybrid model accuracy.



Fig. 2. Preparations of test specimens FRP sheets GFRP, BFRP, CFRP and confinement done

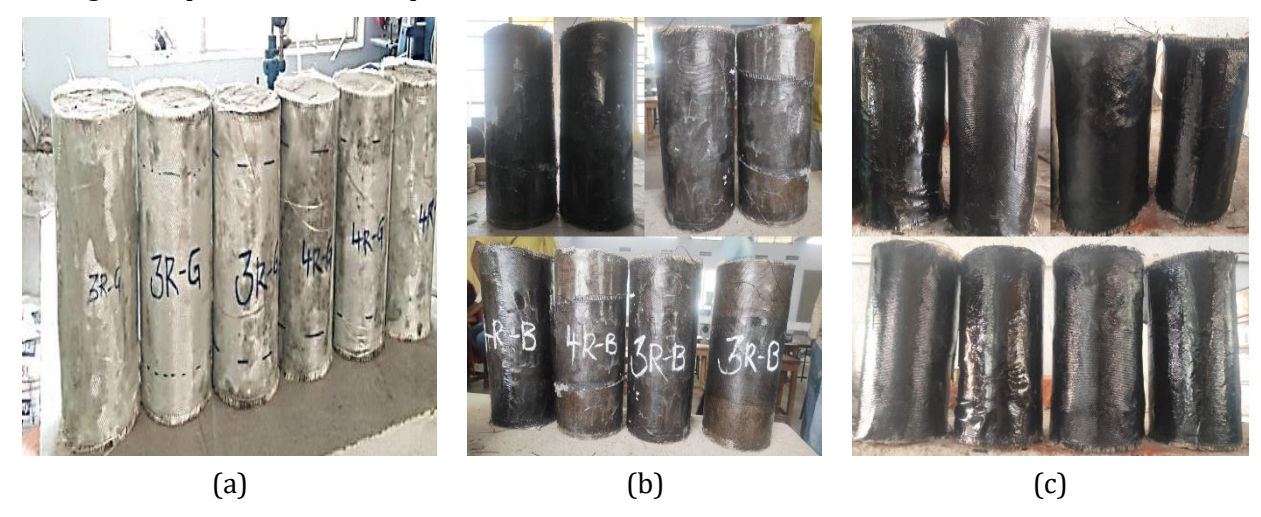


Fig. 3. Wrapped and unwrapped specimens: a) GFRP wrapped specimens 3RG,4RG b) BFRP wrapped specimens. (3RB, 4RB) CFRP wrapped specimens. (3RC, 4RC)

3. Methods

The cylinders were capped using neat Portland cement paste and were tested for compression and split tensile strength according to the guidelines outlined in codes IS:516 [49]. For the compression test specimens, a compress meter was used to record the deflection readings, which were then used to generate stress vs. strain graphs. Cylinders were tested under load control at a uniform rate of 4.1 kN/s (equivalent to 14 MPa/min) as per IS 516 [49]. The compress meter (gauge length = 200 mm; accuracy \pm 0.002 mm) recorded axial deformation concurrently at each load increment. As the load increases, the cylinder eventually fails, and the breaking load is the load at which failure occurs. The failure criterion was defined as the peak axial load corresponding to the maximum compressive stress (f'cc) and its associated axial strain (ϵ at f'cc). This approach, consistent with Lam and Teng [46] and Zhao et al. [21], avoids ambiguity associated with rupture or post-peak strain values.

Overall, the experimental program was developed to achieve statistical reliability, methodological transparency, and practical relevance. The chosen parameters aggregate replacement level, FRP type and layer count, and tie configuration form a coherent and scalable framework for developing sustainable, high-performance recycled aggregate concrete systems under hybrid FRP confinement.

4. Results and Discussion

4.1 Results and Discussion on Analysis of The Impact of Various FRP Types on The Confined and Unconfined Compression Members

Failure modes transition from brittle crushing in unconfined specimens to ductile rupture in those confined with FRP, indicating effective lateral restraint. The unconfined control specimens failed in a brittle compression-splitting mode (Fig. 4), characterized by vertical cracks propagating along the height and crushing of the concrete surface at mid-height. The brittle failure confirmed the lack of lateral restraint. In contrast, the GFRP-confined specimens (Fig. 5) exhibited localized rupture and longitudinal tearing of the fibre jacket around the mid-height region, where lateral dilation was most pronounced.



Fig. 4. Failure mode of unconfined RAC control specimen under axial compression (brittle splitting)



Fig. 5. Failure mode of GFRP-confined RAC specimen (longitudinal tearing, partial delamination)



Fig. 6. Failure mode of BFRP-confined RAC specimen (uniform hoop cracking, fibre splitting)



Fig. 7. Failure mode of CFRP-confined RAC specimen (mid-height rupture band, ductile behaviour)

The debonding of the epoxy interface and no abrupt breakdown showed a gradual progression of the failure, which is moderate in nature. The distributed cracking and circumferential fibre breaking, basalt fibre splitting and localized delamination areas were observed in the BFRP-confined cylinders (Fig. 6). Such trends indicate the presence of uniform confinement pressure and effective energy dissipation, which validates the effectiveness of the BFRP to increase ductility. The CFRP-confined specimens (Fig. 7) demonstrated the most stable and efficient confinement behaviour, where failure was initiated through a narrow rupture band at mid-height, corresponding to the zone of maximum hoop strain. The carbon fibres fractured cleanly without

explosive spalling, and the concrete core remained largely intact, indicating excellent bond adhesion and full mobilization of confinement.

The failure patterns in Figures 4–7 show the transition from brittle splitting in unconfined recycled aggregate concrete (RAC) to ductile rupture in fibre-reinforced polymer (FRP)-confined specimens. The glass fibre-reinforced polymer (GFRP) exhibited longitudinal tearing, the basalt fibre-reinforced polymer (BFRP) exhibited fibre splitting, and the carbon fibre-reinforced polymer (CFRP) failed through mid-height rupture, indicating hoop stress mobilization. This transformation from explosive to gradual failure proves the effectiveness of FRP and hybrid confinement in strain energy dissipation.

4.1.1 Compressive Strength Enhancement under FRP and Tie Confinement

Table 6 and Figure 8 summarize the measured compressive strengths of natural aggregate concrete (NAC-100 %) and recycled aggregate concrete (RAC-50 %) specimens under different confinement configurations. Each value represents the mean of three replicates, with error bars showing \pm 1 SD. The unconfined NAC-100 % and RAC-50 % specimens (N-0 and R-0) recorded average compressive strengths of 34.3 MPa and 30.2 MPa, respectively. The RAC mixture showed a 12 percent decrease than the NAC control mainly due to the existence of attached mortar and elevated porosity and a weaker interfacial transition area (ITZ) in the recycled aggregates.

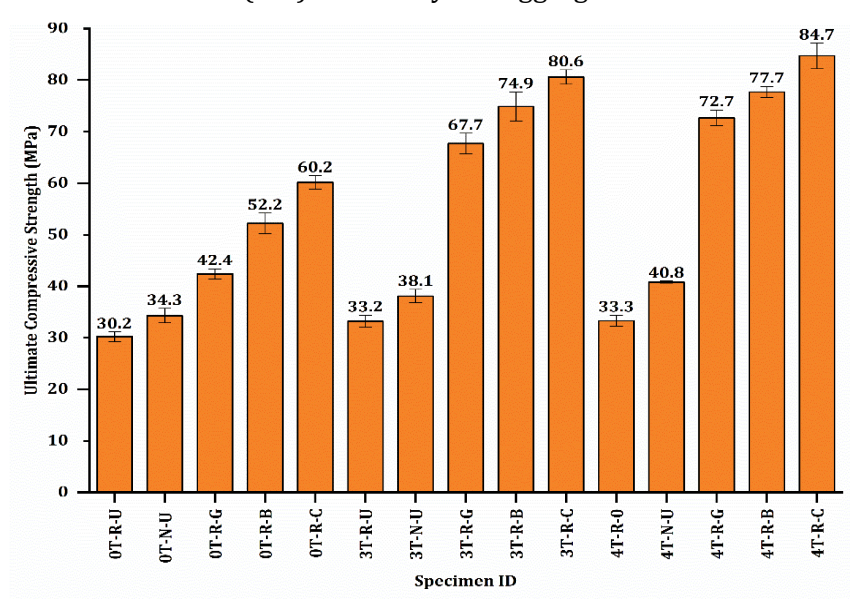


Fig. 8. Ultimate compressive strength of NAC-100 % and RAC-50 % specimens with varying FRP types and number of lateral ties (s = 100 mm and 67.5 mm). Error bars represent $\pm 1 \text{ SD}$; stress in MPa

The mean compressive strengths for the FRP-only RAC-50 % specimens were 42.4 \pm 1.0 MPa (GFRP), 52.2 \pm 2.0 MPa (BFRP), and 60.2 \pm 1.3 MPa (CFRP), compared to 30.2 \pm 0.9 MPa for the unconfined control. The low standard deviations (SD \leq 2 MPa) confirm reliable experimental repeatability. Similarly, for hybrid confinement with three ties, mean strengths were 67.7 \pm 2.0 MPa (GFRP), 74.9 \pm 2.8 MPa (BFRP), and 80.6 \pm 1.4 MPa (CFRP). With four ties, the mean strengths increased marginally to 72.7 \pm 2.0 MPa, 77.7 \pm 1.9 MPa, and 84.7 \pm 1.7 MPa, respectively. These results verify that the observed performance hierarchy remains statistically consistent across configurations, with SD values well within expected variability for confined concrete tests.

The comparative analysis indicates a clear hierarchy among the FRP systems: CFRP > BFRP > GFRP in terms of confined compressive strength. This sequence mirrors the respective fibre moduli and hoop stiffness. However, the strength of the differential narrows as tie density increases. With three ties, the incremental gain from CFRP over BFRP is smaller than in the FRP-only specimens, and at four ties the improvement largely saturates, demonstrating that tie spacing progressively dominates confinement efficiency. Hence, FRP stiffness governs performance in single-mechanism

confinement, whereas hybrid confinement effectiveness is governed primarily by the volumetric steel ratio.

4.1.2 Comparative Stress-Strain Behavior of FRP And Tie Configuration

Figures 9–11 collectively illustrate the evolution of the axial stress–strain response from unconfined to FRP- and hybrid-confined RAC cylinders. The unconfined specimens exhibited a steep ascending branch with abrupt post-peak softening, typical of brittle failure. Once externally wrapped, the RAC displayed a distinct bilinear curve, reflecting progressive activation of lateral confinement and improved energy absorption capacity.

Among the three FRP systems, CFRP consistently demonstrated the highest compressive strength and the most pronounced strain-hardening region, owing to its superior elastic modulus and hoop stiffness. BFRP produced a balanced combination of strength and ductility, while GFRP exhibited modest improvement due to its lower stiffness. The transition from FRP-only confinement to hybrid confinement with three and four ties (s=100~mm and 67.5 mm) further enhanced both strength and deformation capacity. Internal steel ties restrained early dilation, enabling the external FRP to mobilize higher hoop stress at larger strains. As tie density increased, the stress–strain curves exhibited longer plateau regions, confirming effective stress redistribution and improved confinement uniformity. The hierarchical trend CFRP > BFRP > GFRP was observed consistently across all tie configurations; however, the strength difference narrowed under denser tie spacing, indicating that the confinement efficiency is governed increasingly by the volumetric steel ratio rather than FRP stiffness alone.

The transition in fracture patterns from longitudinal splitting in FRP-only specimens to shorter, closely spaced cracks in hybrid systems reflects the interplay between ITZ micro-cracking and hoop-stress redistribution. In recycled aggregate concrete, pre-existing micro voids and weak old-mortar ITZs initiate early lateral dilation. Once confinement is applied, the FRP restrains this dilation, generating hoop tension that redistributes circumferential stress. Lower-modulus jackets (GFRP, BFRP) spreads stress gradually, producing diffuse fracture zones, whereas the higher stiffness of CFRP concentrates hoop stress into a distinct mid-height rupture band. The steel ties shorten the unrestrained dilation length, leading to more uniform crack spacing and delaying FRP rupture.

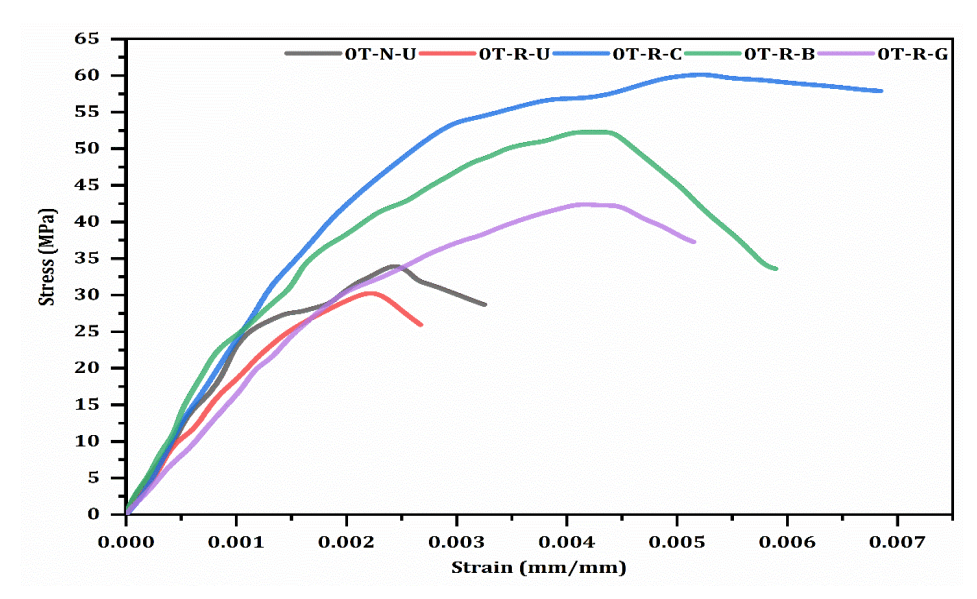


Fig. 9. Stress-strain curves of RAC-50 % cylinders externally confined with two-layer GFRP, BFRP, and CFRP (no ties). Axial stress (MPa) vs. axial strain (mm/mm)

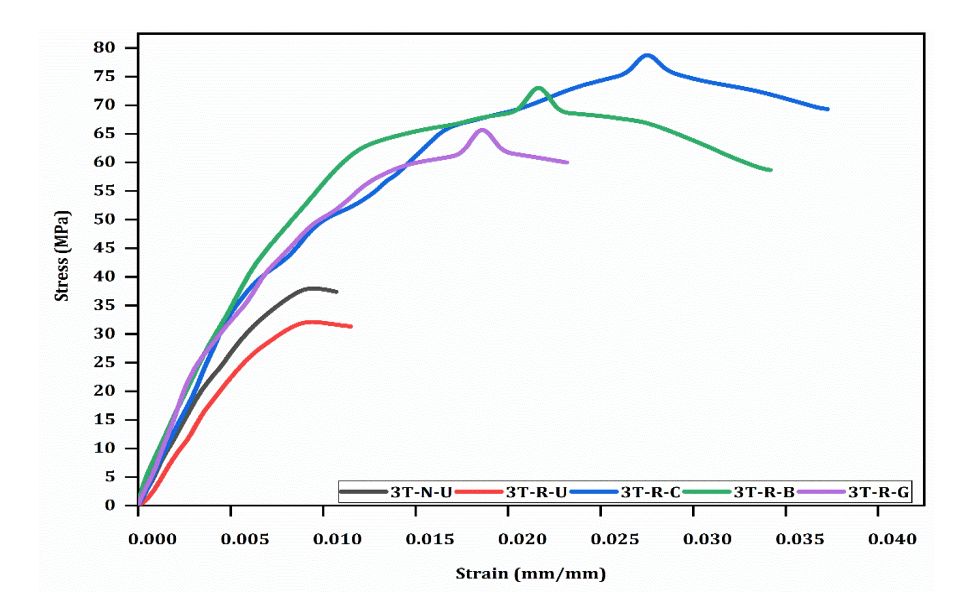


Fig. 10. Stress–strain curves of RAC-50 % cylinders with three steel ties (s = 100 mm) combined with two-layer FRP confinement

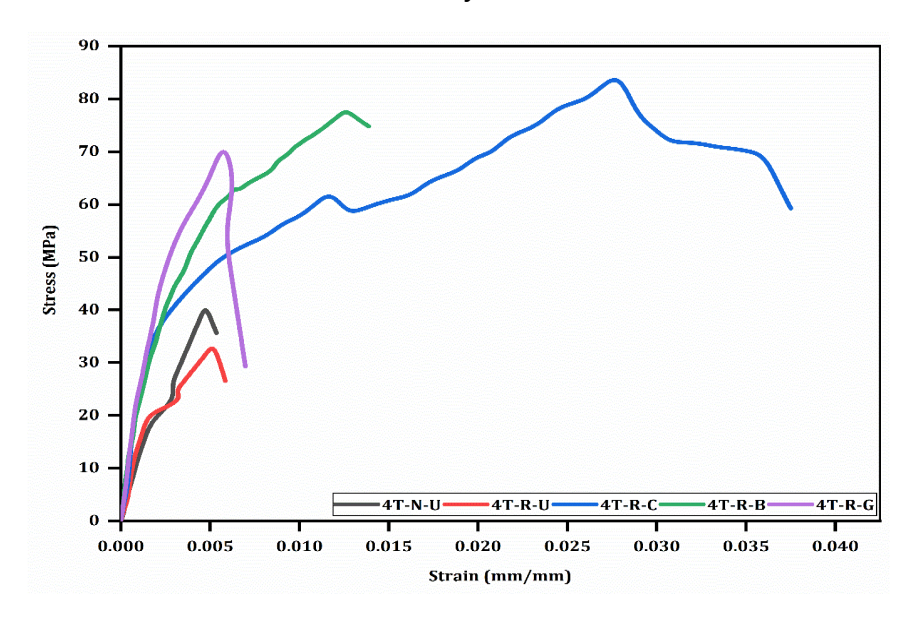


Fig. 11. Uniaxial stress-strain curves of RAC-50 % cylinders with four steel ties (s=67.5mm) combined with two layer FRP confinement

4.1.3 Ultimate Strain and Ductility Trends

The comparative ductility results are presented in Figure 12, where ultimate strain (ϵ at f'cc) is plotted for all confinement systems. Unconfined RAC exhibited ϵ = 0.00218 mm/mm, which is a little less than that of NAC-100 % (0.00246, 13 per cent higher), confirming the more brittle behavior of RAC under microcracking and weaker ITZ. In externally confined wrapping with FRP wraps and no lateral ties the behavior with different fibre types differs. E-glass wrapping brought the strain to 0.00140 (36 % less than unconfined RAC), and the CFRP confinement also decreased to a slightly lower value of 0.00175 (20 % less). BFRP confinement on the other hand increased the strain to 0.00443, which is an augmentation of 103 percent. These findings suggest that fibre stiffness is not a sufficient condition to promote strain increase without steel ties and only BFRP brought significant improvement in ductility response in the experiment.

When three lateral ties were added, the ductility was greatly increased. Unwrapped RAC-50 percent was 0.00902 which was four times higher than the unconfined control. The same was further enhanced when it was combined with FRP wraps: 3R-GFRP = 0.0186 (754 % increase over

unconfined RAC), 3R-BFRP = 0.0217 (896 % increase), and 3R-CFRP = 0.0275 (1162 % increase). Equally, four lateral ties gave RAC-50 % a value of 0.00516 which is already greater than the unconfined figure. This was increased to 0.00580 as applied by external confinement in GFRP (166 % increase), 0.0126 in BFRP (478 % increase) and CFRP (1185 % increase).

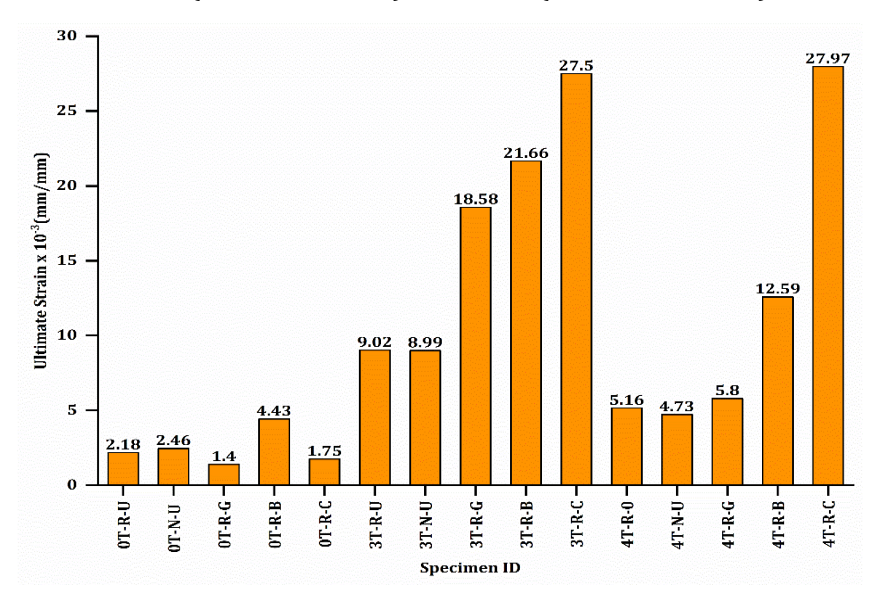


Fig. 12. Ultimate axial strain (ε at f'cc) of RAC-50 % specimens under various FRP and tie configurations. Strain in mm/mm

The results affirm that a combination of FRP confinement and internal steel ties is paramount to mobilization of important ductility in RAC. Among the fibres, CFRP consistently delivered the highest strain enhancement when combined with ties, followed by BFRP, while E-glass provided modest gains. Notably, the strain in 4R-CFRP specimens was more than twelve times greater than that of unconfined RAC, underscoring its superior confinement efficiency.

BFRP consistently provided high strain gains (400–900 %) due to its balanced modulus and rupture strain, whereas GFRP achieved moderate ductility enhancement at lower cost. These findings underline that FRP stiffness alone does not govern ductility; the combined restraint from internal ties and uniform hoop stress distribution is crucial.

The measured results exhibited coefficients of variation (COV) of approximately $3-5\,\%$ for compressive strength and $10-15\,\%$ for ultimate strain, confirming good experimental repeatability. The higher scatter in strain is attributed to heterogeneous ITZ quality and variable bond continuity in recycled aggregates, which influence local hoop strain development. These COV values align with those reported for other RAC confinement studies and validate the reliability of the present dataset.

4.2 Analytical Prediction Using Modified Lam and Teng Model

A recent study aimed at enhancing the design-focused stress-strain model initially introduced by Lam and Teng for FRP confined concrete under axial compression [4] has led to two revised versions of Lam and Teng's model. The first revision updates only the equations for ultimate axial strain and compressive strength. The second revision addresses stress-strain curves that feature a descending branch, which the original model does not accommodate.

4.2.1 The Model Overview

In this study, the bilinear stress–strain model of Lam & Teng [46] was adopted, incorporating the design-oriented refinements of Teng et al. [4] with the results summarized in Table. The lateral confinement pressure was computed using manufacturer-supplied FRP properties thickness, modulus, and effective hoop strain (taken as $0.55 \, \epsilon_f (\mu_0)$). The confinement ratios were computed as

$$\rho_k = \frac{2E_f(nt)}{(f_{cc}^t/\epsilon_{co})D} \quad and \, \rho_\epsilon = \frac{\epsilon_{fu}}{\epsilon_{co}} \tag{1}$$

The confined strength and strain were obtained from

$$\frac{f_{cu}}{f_{co}^{1}} = 1 + 3.5(\rho_k - 0.01)\rho_{\epsilon} \text{ and } \frac{\epsilon_{cu}}{\epsilon_{co}} = 1.75 + 6.5 * \rho_k^{0.8} * \rho_{\epsilon}^{1.45}$$
 (2)

Strength enhancement was obtained through and strain enhancement through

$$f_{cc} = f_{co} + k \times f_1 \tag{3}$$

$$\epsilon_{cc} = \epsilon_{co} \left(1 + k_2 \frac{f_1}{f_{co}} \right) \tag{4}$$

where k_1 = 3.5 and k_2 = 6.5 were adopted from Teng et al. [4]. These coefficients were used in the specimen-wise predictions summarized in Table 8 and verified in the Excel dataset (columns K_1 and K_2). Because the model was originally calibrated for normal concrete with uniform ITZ and continuous FRP wrap, its direct use for RAC may introduce bias. The absence of direct FRP tensile testing further adds uncertainty to Ef and ϵ fe estimates. The steel component followed Mander et al. [45]:

$$\rho_{s} = \frac{4*A_{sh}}{s*d_{s}}; f_{l,steel} = 0.5 * \rho_{s} * f_{yh}.$$
 (5)

Where d_s = core diameter to hoop center line and s= spacing and $A_{sh} = \frac{\pi * d_b^2}{4}$ and f_{yh} =500Mpa, For 8 mm diameter ties (As = 50.27 mm²) and a 92 mm core, the calculated values were: ρs = 2.19 % and fl,steel = 5.46 MPa (for s = 100 mm), and ρs = 3.28 % and fl,steel = 8.20 MPa (for s = 67.5 mm).

4.2.2 FRP Confinement

The lateral confinement pressure provided by the FRP was obtained using the thin-walled cylinder assumption [4]. The FRP contribution computed using the design effective strain ϵ h.rup is the effective hoop strain mobilized at failure. Supplier-certified data were used for Ef and ϵ fu, and the effective strain was computed as:

$$\varepsilon_{h,rup=K_e*\varepsilon_{fu}} \tag{6}$$

A reduction factor ke = 0.586 was adopted in line with ACI 440.2R[47].

$$f_{l.FRP} = \frac{2ntE_f \epsilon_{h,rup}}{D} \tag{7}$$

For hybrid confinement, the total lateral pressure was taken as a direct superposition and approach aligns with prior hybrid confinement models [4, 27].

$$f_{l,tot} = f_{l,FRP} + f_{l,steel} \tag{8}$$

This approach allowed direct comparison of FRP-only and hybrid confinement cases. Model performance was quantified by comparing predicted and experimental values of confined strength and ultimate strain across all groups. The error for each specimen was defined as

$$\%\Delta f = \frac{f_{cu,pred} - f_{cu,expt}}{f_{cc,exp}^{1}} \times 100 \text{ and } \%\Delta \epsilon = \frac{\epsilon_{cu,pred} - \epsilon_{cu,exp}}{\epsilon_{cu,exp}} \times 100$$
 (9)

Bias (mean error), RMSE, and scatter (standard deviation) were then computed on these errors. The results are summarized in Table 8, which reports statistics for each group (RAC/NAC × ties × FRP) and overall.

4.2.3 Example Calculation

For a specimen confined with 8 mm ties at 100 mm spacing, two CFRP layers (t_f = 0.17 mm, E_f = 230 GPa, ϵ_{fu} = 0.015, f'_{co} = 32.1 MPa, and ϵ_{co} = 0.009:

- $\varepsilon_{h,rup} = 0.586 \times 0.015 = 0.00879$
- fl,FRP = $(2 \times 2 \times 0.17 \times 230000 \times 0.00879) / 150 = 9.16 \text{ MPa}$

- fl,steel = 5.46 MPa and fl,total = 14.62 MPa:
- $\rho_k = 2 \times 230000 \times (2 \times 0.17) / (32.1/0.009) \times 150) = 0.2923$ and $\rho_{\epsilon} = 0.015/0.009 = 1.66$
- $f_{cu (pred)} = 32.1[1+3.5(0.02923-1)1.66] = 35.68MPa$
- $\varepsilon_{\text{cu (pred)}} = 0.009 \text{ x } (1.75 + 6.5 \text{ x } (0.2923)^{0.8} \text{ x } (1.66)^{1.45}) = 0.06135 \text{mm/mm}$

The specimen-wise comparison of experimental and predicted confined strength from the Lam-Teng model with Teng et al. [4] and strain is given in Table 8, which reports baseline concrete properties, predicted responses, experimental results, and percentage errors. To facilitate an overall assessment of model performance, Table 9 summarizes the statistical measures of bias (mean error), RMSE, and scatter for both strength and strain, presented separately for CFRP, BFRP, and GFRP, as well as for the total dataset.

Table 8. Specimen-wise comparison of experimental and predicted confined strength and strain for RAC specimens confined with CFRP, BFRP, and GFRP under 0, 3, and 4 ties

Spec. ID	Wrap	T i e s	f_{cc}^1	$rac{arepsilon_{co}}{ ext{mm/m}}$	f _{cc,,exp} (MPa)	$arepsilon_{cu,exp} \ ext{mm/mm}$	$ ho_k$	$ ho_{arepsilon}$	f _{l,FRP} (MPa)	f_{cc}^{1} (MPa)	f _{l,total} (MPa)	€ _{cu.pred} mm/m m	Streng th. Error (%)	Strain Error (%)
3T-R-C	CFRP	3	32.1	0.0090	80.6	0.0275	0.2924	1.663	9.1	85.0	14.6	0.0616	5 %	124 %
3T-R-B	BFRP	3	32.1	0.0090	74.9	0.0217	0.0841	1.884	2.9	47.8	8.4	0.0360	-36 %	67 %
3T-R-G	GFRP	3	32.1	0.0090	67.7	0.0186	0.0860	2.328	3.7	52.0	9.2	0.0438	-23 %	136 %
4T-R-C	CFRP	4	33.3	0.0052	84.7	0.0280	0.1614	2.904	9.1	84.6	17.3	0.0456	0 %	63 %
4T-R-B	BFRP	4	33.3	0.0052	77.7	0.0126	0.0464	3.291	2.9	47.3	11.1	0.0252	-39 %	101 %
4T-R-G	GFRP	4	33.3	0.0052	72.7	0.0058	0.0474	4.066	3.7	51.1	11.9	0.0314	-30 %	442 %
0T-R-C	CFRP	0	30.3	0.0022	42.4	0.0017	0.0748	6.889	9.1	77.7	9.1	0.033	83 %	1788 %
0T-R-B	BFRP	0	30.3	0.0022	52.2	0.0044	0.0215	7.808	2.9	39.8	2.9	0.0167	-24 %	278 %
0T-R-G	GFRP	0	30.3	0.0022	42.4	0.0014	0.0220	9.645	3.7	42.6	3.7	0.0216	1 %	1444 %

Table 9. Statistical evaluation of model performance for FRP-confined RAC specimens. Bias (mean error), RMSE, and scatter for CFRP, BFRP, and GFRP groups and the total dataset, for both strength and ultimate strain predictions

Metric	Wrap	Bias (%)	RMSE (%)	Scatter (%)
	CFRP	-7 %	25 %	21 %
Strength	BFRP	-1 %	28 %	20 %
	GFRP	20 %	50 %	56 %
Total Strength Bias		-7 %	36 %	38 %
	CFRP	109 %	113 %	37 %
Strain	BFRP	202 %	264 %	209 %
	GFRP	1170 %	1337 %	791 %
Total Strain Bias		494 %	789 %	653 %

The predictive capability of Lam-Teng confinement model, with a combination of refinements proposed by Teng et al. [4], was tested with respect to the experimental results of RAC specimens confined with CFRP, BFRP and GFRP at varying level of internal restraint (Table 8). Overall, the general strength trends were represented in the model with a reasonable degree of precision. Nevertheless, significant differences were found in the predictions of strains.

On the compressive strength, the model overpredicted the confined strength of CFRP and GFRP jackets with the BFRP-confined specimens being more in line with the experiment. The bias means of the CFRP and GFRP cases was about -7 % and +20 compared to -1 % of the BFRP cases, which showed that the model slightly underestimated the CFRP strength and slightly overestimated the

GFRP strength, but was not biased in respect to BFRP. The low values of scatter (\leq 21) and RMSEs 25-50 % indicate a stable pattern in prediction of different FRPs (Table 9).

As an illustration, the predicted strength of the 3T-R-C specimen at three ties was 85 MPa, which is equivalent to the measured strength of 80.6 MPa (error margin of about 5 percent), on the other hand, the model strength of the 3T-R-G was 52 MPa, which is equivalent to the measured strength of 67.7 MPa (error margin of about 23 percent). On the same note, regarding the unwrapped cases, the model slightly overestimated the CFRP strength (42.4 - 77.7 MPa, +83 %) but was quite precise when it came to GFRP (42.4 - 42.6 MPa, +1 %) and conservative in the case of BFRP (52.2 - 39.8 MPa, -24 %). These findings prove that Lam-Teng model remains valid in the strength assessment of FRP-confined RAC especially when the confinement pressure is moderate and the FRP strain mobilizes well. On the contrary, final strain forecasts were highly overestimated in all the FRP types. According to the values given in Table 9, the strain bias average was +109 % in CFRP, +202 % in BFRP, and +1170 % in GFRP with equally large RMSE values (113-1337 %). Overestimation trend has continued regardless of the number of ties or levels of confinement. As an example, the OT-R-C specimen was predicted to have an ultimate strain of 0.033 mm/mm and the actual strain was 0.0017 mm/mm (about 1788 higher), but 4T-R-G had a strain error of 442 %. These huge deviations highlight the small ability of the model to replicate the real post-peak deformation properties of FRP-confined RAC.

The main cause of this discrepancy is the fact that the material heterogeneity and lower confinement in RAC are inherent as compared to the natural aggregate concrete. In recycled aggregates, there is the formation of existing microcracks, weak interfacial transition zones (ITZs), and asymmetrical hoop strain growth, which causes premature debonding of FRP and non-uniform growth of tensile strain capacity of the FRP. The Lam-Teng model, which was originally calibrated for normal concrete, consequently overpredicts the lateral dilation and strain capacity when applied to RAC, as it does not account for the early stiffness degradation and aggregate-mortar detachment typical of recycled mixes. Therefore, while the strength prediction component of the Lam-Teng model with Teng et al. [4] refinements remain robust for RAC confined with BFRP, its strain prediction module requires modification. A possible improvement involves introducing a RAC-specific reduction coefficient for the dilation parameter (ke) or employing more advanced confinement models such as those of Ozbakkaloglu and Wu et al. [26, 27], which better represent nonlinear FRP mobilization and strain degradation mechanisms in composite-confined recycled aggregate concretes. Future work will extend the current database to refine the model parameters and enhance the strain prediction accuracy of FRP-confined RAC systems under combined steel and FRP confinement.

4.3 Evaluation of Model Predictions Against Experimental Results

Throughout this study, ultimate strain is defined as the axial strain at peak compressive stress (f_{cc}^1) , not at FRP rupture or percentage branch. All values and models refer to this consistent definition. Figures 13-14 compare predicted versus experimental values. Strength predictions align closely along the 45° line, whereas strain points lie above it, illustrating systematic overestimation. The discrepancy arises from nonuniform confinement and microcracking within RAC, which limit strain mobilization compared with normal concrete. In OT-R-CFRP the ultimate strength was significantly overestimated by the model (by about 83 percent), but the predicted strain (33.3x10⁻³) was much greater than the experimental one (1.7×10^{-3}) , a phenomenon suggesting that the model was overly ductile. On the other hand, OT-R-BFRP was significantly underestimating the strength (-24 %), but 0T-R-GFRP was almost exact on the strength (+0.5 %) though significantly overestimating strain, which is again indicative of the challenge of simulating unconfined or weakly confined recycled aggregate concretes. In the case of three tie specimens, the confinement effects were better represented, but the model remained mixed in its accuracy. In the case of 3T-R-CFRP, there was a minor overestimation of some 5 % but on the other hand, the 3T-R-BFRP and 3T-R-GFRP strengths were overestimated by 36 % and 23 %, respectively. Although the strength patterns improved, final strains were once again grossly underestimated by about 2-3 times less than the experimental values indicating that the model is not very effective in realistic post peak deformation. The fourtie specimens exhibited maximum consistency in the predictions of the strength. The 4T-R-CFRP

strength exactly matched the experimental value, whereas the 4T-R-BFRP and 4T-R-GFRP strengths were underpredicted by 39 % and 30 %, respectively. However, the strain predictions for all 4T configurations remained substantially higher than the measured data, confirming the systematic overprediction of ductility.

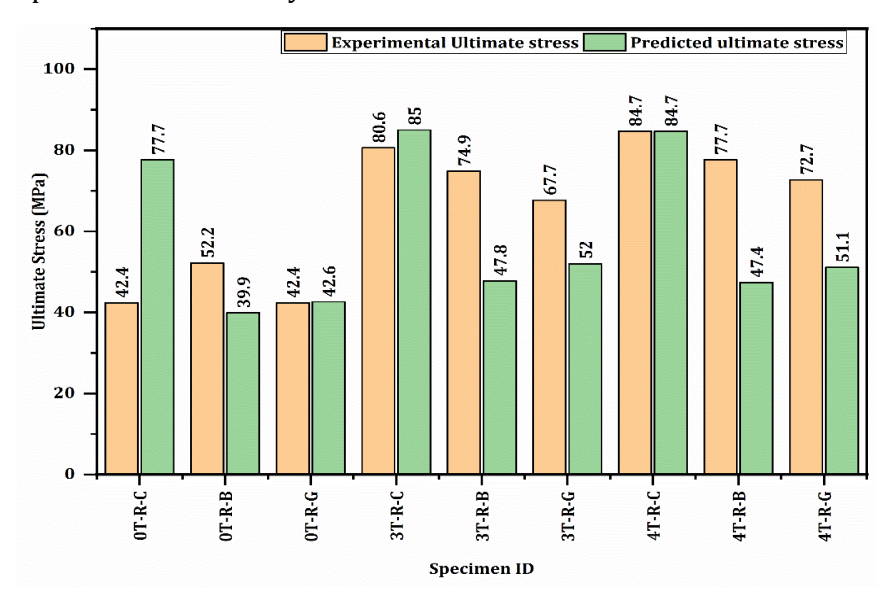


Fig. 13. Predicted vs. experimental compressive strengths (MPa) for FRP-confined RAC cylinders using the modified Lam-Teng model

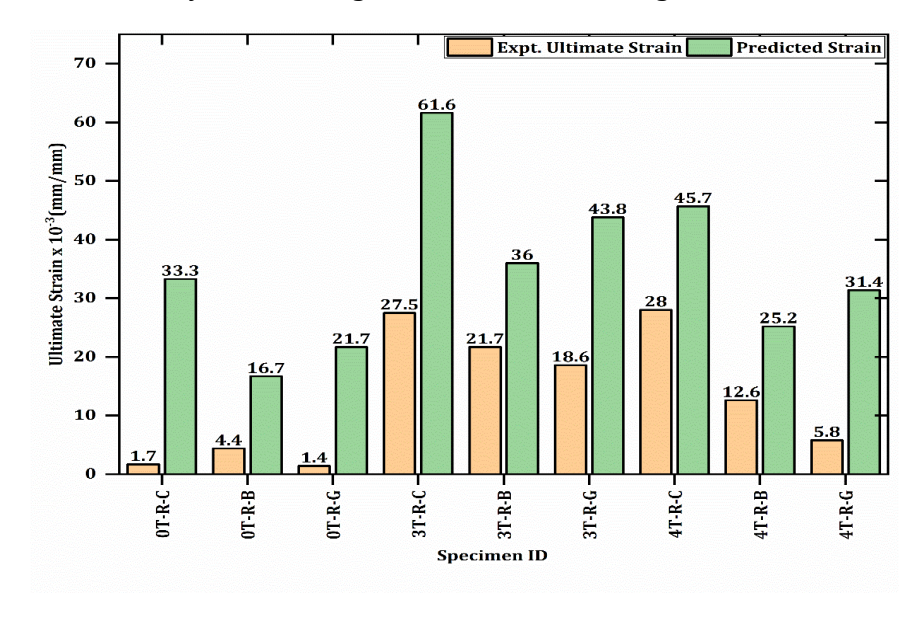


Fig. 14. Predicted vs. experimental ultimate strains (mm/mm) showing model overestimation

The analytical model reproduced the confined strengths within experimental Standard deviation 2MPa for compressive strength, yet consistently over-predicted ultimate strains. This behaviour stems from material heterogeneity and local interface failure mechanisms. In RAC, early ITZ cracking triggers nonuniform lateral dilation, causing the FRP and epoxy to debonding locally and reducing the effective hoop strain that can be mobilized. Because the Lam–Teng formulation assumes uniform confinement and full FRP strain utilization, it provides an upper-bound estimate of ductility. The systematic over-prediction thus reflects physical limitations rather than computational error, highlighting the need for RAC-specific confinement coefficients. Overall, the model successfully captured the trend of strength enhancement with increased tie confinement, but its accuracy varied with the fibre type and tie configuration. The consistent over-prediction of strain across all cases suggests the need for refined calibration of the constitutive parameters, particularly for recycled aggregate concretes under hybrid FRP confinement.

4.4. Conclusion from Analytical Study

The analytical evaluation using the modified Lam and Teng confinement [46] bilinear stress–strain model, refined by Teng et al. [4], demonstrated that the predicted and experimental strength trends of FRP-confined recycled aggregate concrete (RAC) were in close agreement, with mean bias values of –7 % for CFRP, –1 % for BFRP, and +20 % for GFRP. The model was very successful at modelling compressive strength improvement but had a consistent overestimation of the ductility as the strain prediction biases were +109 per cent for CFRP, +202 per cent for BFRP and +1170 per cent for GFRP. The causes of these deviations include the heterogeneous microstructure and the less strong interfacial transition areas in the RAC that decreases the actual mobilization of the FRP strain. Across all confinement systems, the improvement hierarchy follows: CFRP > BFRP > GFRP, with corresponding increases in strength, ductility, and energy absorption. The hybrid configuration with four ties and CFRP wraps delivered the highest performance, achieving up to 84.7 MPa compressive strength and 0.028 mm/mm ultimate strain. The strong correlation between total lateral confinement pressure and axial strain energy capacity confirms the synergistic behaviour between steel and FRP, which should be explicitly considered in future constitutive models for RAC.

4.5 Cost-Performance and Sustainability Analysis

To ensure comparability among different confinement systems, all cost data were normalized to a common performance-based metric of cost per unit strength gain (₹/MPa) relative to the unconfined RAC control. This normalization avoids bias due to differing FRP unit prices and directly represents the strengthening efficiency of each system. To establish cost–performance metrics, typical 2025 Indian market rates were considered as ₹ 3500 /m² for CFRP, ₹ 1800 /m² for BFRP, and ₹ 1200 /m² for GFRP sheets. Each 150 × 300 mm cylinder required about 0.15 m² per layer, giving total two-layer costs of ₹ 1050 (CFRP), ₹ 540 (BFRP), and ₹ 360 (GFRP).

4.5.1 Normalized Cost Metric

To establish cost–performance metrics, typical 2025 Indian market rates were considered as ₹ 3500 /m² for CFRP, ₹ 1800 /m² for BFRP, and ₹ 1200 /m² for GFRP sheets. Each 150 × 300 mm cylinder required about 0.15 m² per layer, giving total two-layer costs of ₹ 1050 (CFRP), ₹ 540 (BFRP), and ₹ 360 (GFRP). From Table 6, the unconfined RAC strength (R-0) was 30.2 MPa, and the FRP-confined specimens achieved: 0T-R-G = 42.4 MPa (Δ = 12.2 MPa); 0T-R-B = 52.2 MPa (Δ = 22.0 MPa); 0T-R-C = 60.2 MPa (Δ = 30.0 MPa). Hence, the normalized cost per MPa strength gain is: GFRP: ₹360 ÷ 12.2 = ₹29.5/MPa; BFRP: ₹540 ÷ 22.0 = ₹24.5/MPa; CFRP: ₹1050 ÷ 30.0 = ₹35.0/MPa. These values confirm that BFRP provides the most cost-efficient confinement, delivering nearly 90 % of CFRP's strength gain at roughly half its cost.

4.5.2 Sensitivity to Price Variability

To assess the robustness of this ranking, a ± 20 % market fluctuation was applied to the FRP unit prices. Even within these ranges (CFRP $\pm 2800-4200/\text{m}^2$, BFRP $\pm 1440-2160/\text{m}^2$, GFRP $\pm 960-1440/\text{m}^2$), the normalized cost ordering remained largely unchanged. The sensitivity results are summarized in Table 10. Even under unfavorable market conditions, BFRP's normalized cost remains competitive ($\pm 19.6-29.5/\text{MPa}$) and consistently lower than CFRP, demonstrating economic stability across realistic price variations.

Table 10. Sensitivity of normalized cost (₹/MPa) to ±20 % FRP price variation

FRP Type	Base Cost (₹/m²)	Cost per MPa Gain (₹/MPa)	Range (±20 %) (₹/MPa)	Δ Strength (%)	Δ Ductility (%)	Cost per % Ductility Gain (₹/ %)	Relative Rank	Sustainability (embodied carbon / recyclability)
CFRP	3500	35	28-42	99	-20	-5250 (ductility drop)	3 (low-cost efficiency)	Highest embodied CO ₂ ; petroleum- based; excellent mechanical

								durability but poor recyclability.
BFRP	1800	24.5	19.6- 29.5	73	103	5.2	1 (best balance)	Low embodied CO ₂ ; basalt mineral source; good alkali/UV resistance; recyclable as mineral filler.
GFRP	1200	29.5	23.6- 35.4	40	-36	-10 (ductility loss)	2 (economical but limited gain)	Moderate embodied CO ₂ ; low cost; limited durability under aggressive exposure.

4.5.3 Data-Driven Comparison

All cost–performance claims are directly supported by experimental data (Table 6), cost data and normalized calculations (Table 10). For instance, CFRP confinement increased f'cc of RAC-50 % from 30.2 MPa to 60.2 MPa; a gain of 30 MPa. At $\stackrel{<}{}$ 1050 per specimen, this corresponds to $\stackrel{<}{}$ 35/MPa, while BFRP achieved comparable strength at $\stackrel{<}{}$ 24.5/MPa. These quantitative comparisons strengthen the argument that BFRP provides a balanced trade-off between structural efficiency and cost (Table 10).

4.5.4 Global Sustainability Perspective

From a sustainability standpoint, the combined use of 50 % recycled coarse aggregate (RCA) and FRP confinement aligns with global circular-economy frameworks such as EN 15804 [50] and the Global Protocol for Buildings (GPC). RCA reduces embodied carbon in the production stage (Modules A1–A2), while FRP confinement extends service life during the use stage (Modules B2–B5) [51].

CFRP offers the highest strength-to-weight ratio but also the highest embodied energy (PAN-based production). BFRP, derived from basalt rock, exhibits lower embodied carbon and superior alkali and UV resistance, contributing to better durability and recyclability potential. GFRP is economical but has moderate environmental benefits and limited long-term stability under severe exposure. Integrating both the economic and environmental indices (₹/MPa and embodied CO₂ footprint) positions BFRP as the most sustainable and cost-effective confinement option for recycled aggregate concrete elements. Its mineral origin and recyclability provide a lower-impact alternative to petroleum-based CFRP, thereby enhancing alignment with Sustainable Development Goals 9 and 12 (Industry, Innovation, and Responsible Consumption). From sustainability point, all FRP-wrapped RAC specimens contribute to reducing the consumption of virgin materials by reusing demolition waste and extending service life through enhanced durability. In terms of fire performance, FRP composites begin to lose stiffness and strength at approximately 2000C, well below the failure temperature of concrete; therefore, passive protection coatings or cementitious fireproof layers is essential for structural applications [36].

Long-term durability (fire, UV), end-of-life recycling, and resin degradation require attention. FRP epoxy matrices typically soften near 200°C and adhesion reduces under elevated temperatures; protective coatings or cementitious jacketing are recommended for field applications [52]. BFRP and GFRP, in comparison, have superior behavior to high temperature and ultraviolet degradations due to their inorganic glassy structure, and CFRP has higher fatigue resistance and stiffness at cyclic load. Basalt fibres show better alkali stability in humid or marine conditions than carbon or E-glass fibres and therefore BFRP is a desirable choice in terms of long-term stability. Furthermore, basalt fibres are made out of naturally occurring volcanic rock and likely to be reused as non-reactive

mineral filler at the end of life, making them more in line with the concept of a circular economy than carbon fibres, which are made using petroleum precursors [53].

Over its life cycle, CFRP offers the highest strength-to-weight ratio but at significantly higher cost and embodied energy. BFRP offers a strong balance between performance and sustainability, combining substantial confinement efficiency with moderate cost and lower environmental impact. GFRP remains a viable low-cost solution for modest structural upgrades or secondary elements. Hence, from both engineering and sustainability perspectives, BFRP emerges as the most balanced confinement material, providing effective strength and ductility gains at a cost and ecological footprint appreciably lower than that of CFRP, while outperforming GFRP in confinement efficiency.

5. Conclusions

This study examined the axial behavior of 150×300 mm recycled aggregate concrete (RAC) cylinders (50 % RCA) confined with two layers of fibre-reinforced polymer (FRP) wraps carbon (CFRP), basalt (BFRP), and glass (GFRP) and up to four internal steel ties. The findings confirm that hybrid confinement, combining internal steel ties with external FRP jackets, substantially enhances both the compressive strength and ductility of RAC, effectively compensating for its weaker interfacial transition zones (ITZs).

The recycled coarse aggregates exhibited approximately 8–10 % lower specific gravity and about 5 % higher water absorption than natural aggregates. These variations led to an overall density reduction and a 10–13 % decrease in compressive strength of RAC compared with natural-aggregate concrete. While all mechanical properties of RAC satisfied the minimum limits of IS 383 [44], its abrasion and impact values were marginally inferior, consistent with the adhered mortar and higher porosity of recycled aggregates.

Among the investigated materials, CFRP achieved the highest confined strength, while BFRP offered the best balance between strength, ductility, and cost efficiency. For FRP-only systems, compressive strength increased by 40-100 % over unconfined RAC; hybrid confinement raised this improvement to 60-80 %. Ultimate strain increased by up to twelvefold (approximately 1200 %), demonstrating major gains in deformability and energy absorption. As tie spacing decreased, the strength difference among FRP types diminished, confirming that volumetric tie ratio governs confinement efficiency once sufficient FRP stiffness is achieved.

The confined strength and deformation characteristics were predicted using analytical modelling of the refined Lam and Teng bi-linear stress-strain model [4, 46]. Close correlation with the experimental strength results was observed in the performance analysis of the model as the values of bias were small (-7 % CFRP, -1 % BFRP and +20 % GFRP). Nevertheless, there was systematic over-prediction of ductility with strain biases greater than 100 % between fibre types. These deviations indicate the inherent limitations of existing design-based models, indicating that strain and post-peak behavior predictions cannot be successfully performed using RAC-specific calibration factors, particularly considering that microstructural heterogeneity and weaker FRP-matrix bonding in RAC.

The modified Lam–Teng bilinear confinement model captured strength enhancement with good reliability (mean bias approximately +5 %, R^2 = 0.94), but consistently over-predicted ultimate strain (bias > 100 %) due to RAC heterogeneity, nonuniform hoop stress, and premature FRP–epoxy debonding. These limitations highlight the need to recalibrate strain enhancement parameters (k_2) to reflect RAC-specific confinement mechanics rather than conventional concrete assumptions.

From a cost–performance perspective, the normalized strengthening cost of BFRP (approximately $\stackrel{?}{_{\sim}}$ 24.5 / MPa) was roughly half that of CFRP (approximately $\stackrel{?}{_{\sim}}$ 35 / MPa) while achieving 90 % of its performance, establishing BFRP as a technically and economically optimal confinement material. GFRP remained the most economical but delivered moderate ductility gains, suitable for secondary strengthening applications.

Within the scope of this investigation, the combined use of FRP wrapping and steel tie confinement improved the compressive strength of RAC cylinders by up to 60 % and the ultimate strain by nearly twelvefold relative to unconfined specimens. The confinement efficiency followed the order CFRP > BFRP > GFRP, but the overall cost–benefit and sustainability balance indicated that BFRP is the most practical option for the structural strengthening of RAC.

From a sustainability perspective, incorporating 50 % recycled aggregates significantly reduces dependence on natural quarry materials, minimizing carbon emissions, and promotes circular construction practices. FRP wrapping further extends the service life of structural members through corrosion-free confinement; however, environmental challenges remain because of the non-recyclable thermoset epoxy resins used in most FRP systems. Basalt fibres, derived from naturally occurring volcanic rock, offer a sustainable advantage: they can be repurposed as inert mineral fillers at the end of their lifecycle, giving BFRP a lower environmental footprint compared with CFRP, which is derived from petroleum-based precursors. However, durability under extreme conditions remains a design concern: FRP composites begin to lose stiffness at approximately 200°C and epoxy matrices degrade under prolonged ultraviolet exposure. Hence, protective coatings or fire-resistant wraps are recommended for field applications [36, 53].

5.1 Recommendations for Future Work

Further research should extend these findings to larger column geometries, cyclic and fatigue loading, and long-term durability under thermal and UV exposure. Microstructural imaging of ITZ cracking and bond degradation is recommended to support RAC-specific calibration of FRP confinement models, improving predictive accuracy for hybrid systems in sustainable infrastructure design.

5.2 Scope and Limitations

The present investigation was limited to 150 mm × 300 mm circular cylinders containing 50 % recycled coarse aggregate and two layers of full FRP wraps. The results and analytical correlations are therefore applicable only within this scale and material configuration. The study does not extend to rectangular columns, partial wraps, higher or lower FRP layer counts, or long-term durability and creep effects. Further research incorporating FRP-confined NAC specimens, different recycled aggregate replacement ratios, and variable confinement pressures are required to generalize the conclusions for design or field applications. Machine learning (ML) models (like CATO or CATO-MZW) are promising tools for RAC studies and there is a need for large experimental datasets to support ML use.

Acknowledgements

The authors thank the management and Principals of Vasavi College of Engineering, CBIT, Hyderabad and KITS Warangal for the support extended.

References

- [1] Fatiha A, Karim E, Mhamed A, Abed F. Enhancing performance of recycled aggregate concrete with supplementary cementitious materials. Cleaner Materials. 2025;15:100298. https://doi.org/10.1016/j.clema.2025.100298
- [2] Douadi A, Babba R, Hebbache K, Boutlikht M, Nour El Houda K, Abderraouf M, et al. Evaluation of CFRP confinement performance and predictive accuracy of design codes and stress-strain models for concrete. Research on Engineering Structures and Materials (RESM). 2024;11(4):1615-32. https://doi.org/10.17515/resm2024.435me0906rs
- [3] Sangeetha P, Prithvi R, Ashwin Kumaran VM, B, Yaashika M. Structural behavior of deficient hollow steel columns strengthened using GFRP. Research on Engineering Structures and Materials. 2025;Online First. https://doi.org/10.17515/resm2025-541st1121rs
- [4] Teng JG, Jiang T, Lam L, Luo YZ. Refinement of a design-oriented stress–strain model for FRP-confined concrete. Journal of Composites for Construction. 2009;13(4):269-78. https://doi.org/10.1061/(ASCE)CC.1943-5614.0000012
- [5] Berndt ML. Properties of sustainable concrete containing fly ash, slag and recycled concrete aggregate. Construction and Building Materials. 2009;23(7):2606-13. https://doi.org/10.1016/j.conbuildmat.2009.02.011

- [6] Verian KP, Ashraf W, Cao Y. Properties of recycled concrete aggregate and their influence in new concrete production. Resources, Conservation and Recycling. 2018;133:30-49. https://doi.org/10.1016/j.resconrec.2018.02.005
- [7] Xu J-J, Chen Z-P, Ozbakkaloglu T, Zhao X-Y, Demartino C. A critical assessment of the compressive behavior of reinforced recycled aggregate concrete columns. Engineering Structures. 2018;161:161-75. https://doi.org/10.1016/j.engstruct.2018.02.003
- [8] Choi W-C, Yun H-D. Compressive behavior of reinforced concrete columns with recycled aggregate under uniaxial loading. Engineering Structures. 2012;41:285-93. https://doi.org/10.1016/j.engstruct.2012.03.037
- [9] Shatarat N, Alhaq AA, Katkhuda H, Jaber MtA. Investigation of axial compressive behavior of reinforced concrete columns using recycled coarse aggregate and recycled asphalt pavement aggregate. Construction and Building Materials. 2019;217:384-93. https://doi.org/10.1016/j.conbuildmat.2019.05.085
- [10] Wang Q-L, Li J, Shao Y-B, Zhao W-J. Flexural performances of square concrete filled CFRP-steel tubes (S-CF-CFRP-ST). Advances in Structural Engineering. 2015;18(8):1319-44. https://doi.org/10.1260/1369-4332.18.8.1319
- [11] Wang Y, Liang J, Wang C, Li W. Axial compression behavior of carbon fiber reinforced polymer confined partially encased recycled concrete columns. PLOS ONE. 2024;19(6):e0304797. https://doi.org/10.1371/journal.pone.0304797
- [12] Choudhury MSI, Amin AFMS, Islam MM, Hasnat A. Effect of confining pressure distribution on the dilation behavior in FRP-confined plain concrete columns using stone, brick and recycled aggregates. Construction and Building Materials. 2016;102:541-51. https://doi.org/10.1016/j.conbuildmat.2015.11.003
- [13] Suhail R, Amato G, McCrum DP. Active and passive confinement of shape-modified low strength concrete columns using SMA and FRP systems. Composite Structures. 2020;251:112649. https://doi.org/10.1016/j.compstruct.2020.112649
- [14] Muhammad NSH, Thong MP, Lei X. New method of strengthening reinforced concrete square columns by circularizing and wrapping with fiber-reinforced polymer or steel straps. Journal of Composites for Construction. 2013;17(2):229-38. https://doi.org/10.1061/(ASCE)CC.1943-5614.0000335
- [15] Abu-Sena ABB, Said M, Zaki MA, Dokmak M. Behavior of hollow steel sections strengthened with CFRP. Construction and Building Materials. 2019;205:306-20. https://doi.org/10.1016/j.conbuildmat.2019.01.237
- [16] Kim J, Grabiec AM, Ubysz A. An experimental study on structural concrete containing recycled aggregates and powder from construction and demolition waste. Materials. 2022;15(7). https://doi.org/10.3390/ma15072458
- [17] Zhu J-T, Wang X-L, Xu Z-D, Weng C-H. Experimental study on seismic behavior of RC frames strengthened with CFRP sheets. Composite Structures. 2011;93(6):1595-603. https://doi.org/10.1016/j.compstruct.2011.01.007
- [18] Park TW, Na UJ, Chung L, Feng MQ. Compressive behavior of concrete cylinders confined by narrow strips of CFRP with spacing. Composites Part B: Engineering. 2008;39(7):1093-103. https://doi.org/10.1016/j.compositesb.2008.05.002
- [19] Silva RV, De Brito J, Dhir RK. The influence of the use of recycled aggregates on the compressive strength of concrete: a review. European Journal of Environmental and Civil Engineering. 2015;19(7):825-49. https://doi.org/10.1080/19648189.2014.974831
- [20] Dey T, Das CS, Mishra N. Behaviour of confined recycled aggregate concrete under compressive loading: An experimental investigation. Journal of Building Engineering. 2020;32:101825. https://doi.org/10.1016/j.jobe.2020.101825
- [21] Zhao JL, Yu T, Teng JG. Stress-strain behavior of FRP-confined recycled aggregate concrete. Journal of Composites for Construction. 2015;19(3):04014054. https://doi.org/10.1061/(ASCE)CC.1943-5614.0000513
- [22] Sunayana S, Barai SV. Performance of fly ash incorporated recycled aggregates concrete column under axial compression: Experimental and numerical study. Engineering Structures. 2019;196:109258. https://doi.org/10.1016/j.engstruct.2019.05.099
- [23] Chen G, Zhang J, Wu Y, Lin G, Jiang T. Stress–strain behavior of FRP-confined recycled aggregate concrete in square columns of different sizes. Journal of Composites for Construction. 2021;25(5):04021040. https://doi.org/10.1061/(ASCE)CC.1943-5614.0001150
- [24] Deresa ST, Xu J, Demartino C, Heo Y, Li Z, Xiao Y. A review of experimental results on structural performance of reinforced recycled aggregate concrete beams and columns. Advances in Structural Engineering. 2020;23(15):3351-69. https://doi.org/10.1177/1369433220934564

- [25] Zhang LW, Sojobi AO, Liew KM. Sustainable CFRP-reinforced recycled concrete for cleaner eco-friendly construction. Journal of Cleaner Production. 2019;233:56-75. https://doi.org/10.1016/j.jclepro.2019.06.025
- [26] Wu G, Lü ZT, Wu ZS. Strength and ductility of concrete cylinders confined with FRP composites. Constr Build Mater. 2006;20(3):134-48. https://doi.org/10.1016/j.conbuildmat.2005.01.022
- [27] Ozbakkaloglu T, Lim JC. Axial compressive behavior of FRP-confined concrete: Experimental test database and a new design-oriented model. Compos Part B Eng. 2013;55:607-34. https://doi.org/10.1016/j.compositesb.2013.07.025
- [28] Khodadadi N, Roghani H, De Caso F, El-kenawy E-SM, Yesha Y, Nanni A. Data-driven PSO-CatBoost machine learning model to predict the compressive strength of CFRP-confined circular concrete specimens. Thin-Walled Struct. 2024;198:111763. https://doi.org/10.1016/j.tws.2024.111763
- [29] Dada TE, Gong G, Xia J, Di Sarno L. Stress-strain behaviour of axially loaded FRP-confined natural and recycled aggregate concrete using design-oriented and machine learning approaches. J Build Eng. 2024;95:110256. https://doi.org/10.1016/j.jobe.2024.110256
- [30] Nguyen T-H, Vuong H-T, Shiau J, Nguyen-Thoi T, Nguyen D-H, Nguyen T. Optimizing flexural strength of RC beams with recycled aggregates and CFRP using machine learning models. Sci Rep. 2024;14(1):28621. https://doi.org/10.1038/s41598-024-79287-1
- [31] Neupane RP, Imjai T, Makul N, Garcia R, Kim B, Chaudhary S. Use of recycled aggregate concrete in structural members: a review focused on Southeast Asia. J Asian Archit Build Eng. 2025;24(3):1197-220. https://doi.org/10.1080/13467581.2023.2270029
- [32] Zhang X, Dai C, Li W, Chen Y. Prediction of compressive strength of recycled aggregate concrete using machine learning and Bayesian optimization methods. Front Earth Sci. 2023;11:1112105. https://doi.org/10.3389/feart.2023.1112105
- [33] Alsharari F. Predicting the compressive strength of fiber-reinforced recycled aggregate concrete: A machine-learning modeling with SHAP analysis. Asian J Civ Eng. 2025;26(1):179-205. https://doi.org/10.1007/s42107-024-01183-w
- [34] Nadi S, Beheshti Nezhad H, Sadeghi A. Experimental study on the durability and mechanical properties of concrete with crumb rubber. J Build Pathol Rehabil. 2021;7(1):17. https://doi.org/10.1007/s41024-021-00156-9
- [35] Damera H, Dakshina Murthy NR, Ramana Rao NV. Mechanical and durability studies on blended pozzolonic concretes with fly ash & recycled aggregates. Mater Today Proc. 2020;27:1522-9. https://doi.org/10.1016/j.matpr.2020.03.174
- [36] Haris M, Xiong E, Gao W, Samuel MA, Sahar NU, Saleem A. Strengthening reinforced concrete members using FRP—Evaluating fire performance, challenges, and future research directions: A state-of-the-art review. Polymers. 2025;17(1). https://doi.org/10.3390/polym17010013
- [37] Salih MA, Ahmed SK, Alsafi S, Abullah MM, Jaya RP, Abd Rahim SZ, Aziz IH, Thanaya IN. Strength and durability of sustainable self-consolidating concrete with high levels of supplementary cementitious materials. Materials. 2022;15(22). https://doi.org/10.3390/ma15227991
- [38] Hasheminezhad AA, Beheshti Nezhad H, Mahmoodabadi M, Sadeghi A. Predicting the service life of self-compacting concrete under corrosive conditions. J Civil Eng. 2025;15(1):13-20. https://doi.org/10.26634/jce.15.1.21743
- [39] Gedik O. Comparison and enhancement of design procedures for guideline expressions to predict the compressive capacity of FRP-wrapped concrete members. Arab J Sci Eng. 2024;49(10):13559-76. https://doi.org/10.1007/s13369-024-08707-1
- [40] Fan Z, Liu H, Liu G, Wang X, Cui W. Compressive performance of fiber-reinforced recycled aggregate concrete by basalt fiber reinforced polymer-polyvinyl chloride composite jackets. J Renew Mater. 2023;11(4):1763-91. https://doi.org/10.32604/jrm.2023.024319
- [41] Shamass R, Rispoli O, Limbachiya V, Kovacs R. Mechanical and GWP assessment of concrete using blast furnace slag, silica fume and recycled aggregate. Case Stud Constr Mater. 2023;18:e02164. https://doi.org/10.1016/j.cscm.2023.e02164
- [42] Xing W, Tam V, Le K, Hao J, Wang J, Yang P. Life cycle assessment of recycled concrete incorporating recycled aggregate and nanomaterials. In: Nanotechnology in Construction for Circular Economy (NICOM). Singapore: Springer; 2022. p. 491-3. https://doi.org/10.1007/978-981-99-3330-3 50
- [43] Bureau of Indian Standards. IS 269:2015 Ordinary Portland Cement—Specifications (Sixth Revision). New Delhi; 2015.
- [44] Bureau of Indian Standards. IS 383:2016 Coarse and fine aggregate for concrete—Specification (Third Revision). New Delhi; 2016.
- [45] Mander JB, Priestley MJN, Park R. Theoretical stress-strain model for confined concrete. J Struct Eng. 1988;114(8):1804-26. https://doi.org/10.1061/(ASCE)0733-9445(1988)114:8(1804)
- [46] Lam L, Teng JG. Design-oriented stress-strain model for FRP-confined concrete. Constr Build Mater. 2003;17(6):471-89. https://doi.org/10.1016/S0950-0618(03)00045-X

- [47] American Concrete Institute. ACI 440.2R-17 Guide for the Design and Construction of Externally Bonded FRP Systems for Strengthening Concrete Structures. Farmington Hills (MI); 2017.
- [48] Bureau of Indian Standards. IS 10262:2019 Concrete Mix Proportioning—Guidelines (First Revision). New Delhi; 2019.
- [49] Bureau of Indian Standards. IS 516-1-1:2021 Hardened Concrete—Compressive, Flexural and Split Tensile Strength (First Revision). New Delhi; 2021.
- [50] European Committee for Standardization. EN 15804:2012+A2:2019 Sustainability of Construction Works—Environmental Product Declarations—Core Rules for Construction Products. Brussels; 2019.
- [51] Abouhamad M, Abu-Hamd M. Life cycle assessment framework for embodied environmental impacts of building construction systems. Sustainability. 2021;13(2). https://doi.org/10.3390/su13020461
- [52] Cao S, Wu Z, Wang X. Tensile properties of CFRP and hybrid FRP composites at elevated temperatures. J Compos Mater. 2009;43(4):315-30. https://doi.org/10.1177/0021998308099224
- [53] Diniță A, Ripeanu RG, Ilincă CN, Cursaru D, Matei D, Naim RI, Tănase M, Portoacă AI. Advancements in fiber-reinforced polymer composites: A comprehensive analysis. Polymers. 2024;16(1). https://doi.org/10.3390/polym16010002